ELSEVIER

Journal of Power Sources 109 (2002) 377–387

JOURNAL OF POWER SOURCES

www.elsevier.com/locate/jpowsour

Study of polypyrrole graphite composite as anode material for secondary lithium-ion batteries

Basker Veeraraghavan[a], Jason Paul[b], Bala Haran[a], Branko Popov[a,*]

[a]*Department of Chemical Engineering, University of South Carolina, Columbia, SC 29208, USA*
[b]*Department of Chemical Engineering, Brown University, Providence, RI, USA*

Received 28 December 2001; accepted 16 February 2002

Abstract

Pyrrole was polymerized onto commercial SFG10 graphite by in situ polymerization technique. Polymerization decreases the initial irreversible capacity loss of the graphite anode. The decrease in the irreversible capacity loss is due to the reduction in the thickness of the solid electrolyte interface (SEI) layer formed. PPy/C (7.8%) gives the optimum performance based on the irreversible capacity loss and the discharge capacity of the composite. The composite material has been studied for specific discharge capacity, coulombic efficiency, rate capability and cycle life using a variety of electrochemical methods. The composite SFG10 graphite possess good reversibility, higher coulombic efficiency, good rate capability and better cycle life than the bare SFG10 graphite. © 2002 Elsevier Science B.V. All rights reserved.

Keywords: Polypyrrole; Irreversible capacity; Anode material; Lithium-ion batteries

1. Introduction

To ensure long cycle life and safety, different types of carbon including graphite [1] and coke [2] have been studied as anodes for the Li-ion battery. Of various carbon materials that have been tried, graphite is favored because it (i) possesses a high theoretical capacity of 372 mAh/g [3]; (ii) has desirable potential profile for Li-ion intercalation and (iii) is much cheaper than MCMB and also provides good cycle life and safety. However, carbonaceous anodes exhibit capacity loss during the first intercalation step. This is due to the irreversible reactions that take place with lithium at the electrolyte interface. In commercial Li-ion cells this loss in capacity is compensated with the use of excess cathode material. This, however, leads to an increase in the weight of the battery and hence contributes to a decrease in the specific energy density of the cell [4,5]. Therefore, many researchers have focused on reducing the irreversible reactions of graphite without sacrificing its capacity.

In our previous paper, we developed a Sn/C composite, which showed a substantial increase in the reversible capacity as compared to pure graphite [6]. Tin has been shown to possess very high capacity for lithium intercalation [7]. But the main drawback of using tin is that it shows poor cycling characteristics and also gives rise to a large initial irreversible capacity. The ''pulverization'' problems during cycling results in the poor cycling of the anode material and the large irreversible capacity is due to the following reaction during initial cycling:

$$SnO + 2Li^+ \rightarrow Sn + Li_2O$$

$$SnO_2 + 4Li^+ \rightarrow Sn + 2Li_2O$$

In synthesizing the composite material we were able to eliminate the capacity fade problems associated with tin. However, the initial irreversible capacity loss was magnified in the composite material. The composite showed a higher irreversible capacity (350.7) than bare graphite (232.7 mAh/g) due to the irreversible reactions of tin with lithium. Hence, our next objective was to reduce the irreversible capacity associated with the Sn/C composite.

It is widely known that the irreversible capacity loss in carbon originates from the decomposition of the electrolyte on the graphite surface followed by the formation of the solid electrolyte interface (SEI) layer on the external surface of the graphite. This layer is electronically insulating but permeable to Li^+ ions. It is impermeable to other electrolyte components, and is mainly composed of lithium carbonate and lithium alkyl carbonates [8,9], as the electrolyte solvents generally used are alkyl carbonates. The process is irreversible and contributes to the loss in capacity. The irreversible capacity loss can also arise from the solvated intercalation of lithium between the graphene layers and subsequent

* Corresponding author. Tel.: +1-803-777-7314; fax: +1-803-777-8265.
E-mail address: popov@engr.sc.edu (B. Popov).

0378-7753/02/$ – see front matter
PII: S0378-7753(02)00105-2

reduction of the solvent, since the formation of $Li_x(sol)_yC_6$ is favored more than the formation of LiC_6 [10,11]. This process results in the severe degradation of the graphene layers. This process is called 'exfoliation' of graphite. The irreversible capacity loss associated with the use of graphite also varies considerably with different electrolytes, and especially with different solvents. It has been shown that the irreversible reactions are worse in propylene carbonate (PC) based electrolytes than in ethylene carbonate (EC) based electrolytes [12,13]. Since the SEI layer is formed due to the interaction of the electrode with the electrolyte, modifying the electrolyte or the electrode material can control the extent of the irreversible capacity losses.

Recently, modifications to the electrolyte have been tried out to suppress the irreversible solvated lithium intercalation into graphite by adding inorganic agents such as CO_2 [14], NO_2 [15] and SO_2 [16]. These additives contribute to the formation of a less permeable SEI film, which effectively decreases the diffusion of solvated lithium ions through the surface of the graphite. However, these modifications do not decrease the irreversible capacity satisfactorily and also lead to an increase in the deadweight of the battery. Also, such modifications are highly specific to the type of graphite studied and with the same electrolyte composition, some other graphites show high irreversible capacity losses. The electrode surface has also been modified by coating Ni [17] and Pd [18] on the surface. These metals reduce the irreversible capacity losses by reducing the extent of solvated lithium intercalation. But such surface modifications also have a tendency to reduce the reversible capacity of the composites.

Electronically conducting polymers such as polypyrrole, polyaniline and polythiophene have been used in various applications like batteries and supercapacitors [19,20]. Polypyrrole and polyaniline has been used in the case of cathode powders like $LiMn_2O_4$ [21,22] and V_2O_5 [23], in which they serve the dual-purpose of a binder and a conducting additive, thereby reducing the inert weight associated in the preparation of the electrode. For example, in the case of $LiMn_2O_4$–PPy composites, the addition of polypyrrole increases the capacity of the pure $LiMn_2O_4$ from 110 mAh/g to 125 mAh/g over 120 cycles. The polymers form a conducting matrix, which provides a conducting backbone for the particles, thereby improving greatly the conductivity of the electrode by reducing the particle-to-particle contact resistance. This has a direct impact on improving the coulombic efficiency, rate capability and the cycle life of the electrode material. However, testing of the polypyrrole-coated carbon revealed that apart from improving the above-mentioned characteristics, it also decreases the initial irreversible capacity associated with the carbon anodes.

Hence, the objective of this work is to reduce the irreversible capacity loss of bare graphite and Sn–graphite composite by using a polymer additive. First, we developed graphite composite anodes for Li-ion cells by modification treatment based on polymerization of pyrrole. Second, TGA analysis was done to determine the amount of polypyrrole in the synthesized material. Third, graphite with different polypyrrole contents was electrochemically characterized. The reversibility, initial capacity loss, capacity decay with cycling and Li^+ intercalation kinetics were analyzed in detail Finally, similar studies were done on the Sn/C composite polymerized with polypyrrole.

2. Experimental

2.1. Preparation of PPy/C composite

Synthetic graphite, commercially known as SFG10 was used as received from Timcal® America for all the experimental studies. Pyrrole, received from Aldrich, was polymerized in an aqueous slurry of the graphite powders at 0 °C using nitric acid as an oxidizer. About 10 mg of sodium salt of dodecyl benzene sulphonic acid was used as a dopant. Adding appropriate weights of the monomer to 2 g of the graphite powder varied the polypyrrole content in the composites. Before polymerization, the monomer was distilled several times and guarded against exposure to light to prevent residual polymerization. The polymerization was carried out for 40 h with constant stirring. Following the polymerization reaction, the powders were thoroughly washed with water and methanol and dried at 200 °C for 24 h under vacuum.

2.2. Material characterizations

The morphology of the bare and the composite graphite were analyzed using a Hitachi S-2500 Delta Scanning Electron Microscope. Thermo gravimetric analysis (TGA) was done to determine change in sample weight with increase in temperature. Changes in the graphite surface area due to polypyrrole inclusion were studied using Micromeritics Pulse Chemisorb 2700 based on single-point, Brunaeur–Emmett–Teller (BET) method. Each sample was dried in a flowing stream of argon at 200 °C for 1 h prior to BET measurement.

2.3. Electrode preparation and electrochemical characterization

Typical graphite negative electrodes were prepared by adding 50% (v/v) solution of isopropyl alcohol (solvent). No binder was required in the case of the composites, since polypyrrole formed a conducting matrix for the graphite particles, which served in helping to reduce the inert weights associated with the preparation of the electrodes. However, in the case of bare graphite, 10 wt.% of PTFE was added in the form of a solution of 60 wt.% PTFE solution. The resulting slurry was then mixed in an ultrasonic cleaner for 1 h. Pellets of the composite and the bare carbon samples were prepared by cold-rolling technique. Disk electrodes 1.4 cm^2 in area were cut out from the cold pressed material. Electrochemical characterization studies were performed

using a three electrode T-cell set up based on a 0.5 in. perfluoroalkoxy tee (Swagelok). T-cells were prepared in a glove box filled with ultra pure argon (National Gas and Welders Inc.). The electrodes in the T-cells were prepared by cold pressing material on both sides of metal current collectors (MS cylinders). Pure lithium metal was used as the counter and reference electrode. 1M $LiPF_6$ in a 1:1 mixture of EC and dimethyl carbonate (DMC) with less than 15 ppm H_2O and 80 ppm HF (EM Inc.) was used as the electrolyte. Whatman fiber membrane (Baxter Diagnostic Co.) was used as a separator.

Cycling and rate capability studies were carried out using Arbin Battery Test Station (BT-2043) at a current density of 0.25 mA/cm^2 ($\sim C$/15 rate), with the cut-off potentials being 0.005 versus Li/Li$^+$ for discharge and 2 V versus Li/Li$^+$ for charge. In this paper, the discharge capacity of the negative electrode refers to the lithium intercalation capacity while the charge capacity refers to the lithium de-intercalation capacity. Cyclic voltammograms were obtained at a scan rate of 0.05 mV/s using EG&G potentiostat (Model 273A). The complex-impedance analyses were performed using a Solartron 1255 analyzer along with EG&G potentiostat (Model 273A) over a frequency range of 100 kHz to 1 mHz with a signal amplitude of 5 mV peak-to-peak.

3. Results and discussion

3.1. Estimation of the amount of polypyrrole in the composite

The approximate amount of polypyrrole in the composite was determined using Thermo gravimetric analysis. TGA analysis was carried under air to burn the samples, and the temperature was scanned from room temperature to 900 °C at a rate of 5 °C /min. Fig. 1 shows the TGA behavior of the composite samples along with those of graphite and polypyrrole. As seen from the figure, polypyrrole burns off at a temperature of 420 °C, while the bare graphite loses weight rapidly at 900 °C. The composite shows weight losses at these two regions, the first of which corresponds to the burning of polypyrrole, while the second corresponds to the burning of graphite. From Fig. 1, the difference in weight before and after burning polypyrrole can be determined. The change in weight directly translates to amount of polypyrrole in the composite. The amount of polypyrrole, in percentage, was found by subtracting the weight percentage of the bare graphite at 420 °C (100%) and that of the corresponding composite at the same temperature. The key assumption involved in this calculation is that only polypyrrole burns within this temperature range and that this burning accounts for all the weight change. Since the sample corresponding to pure graphite burns only at temperatures greater than 700 °C, this is a valid assumption. Using this method, it was found that the amounts of polypyrrole in the composites varied from 5 to 8.4%.

3.2. Initial cycling behavior of composite graphites

The initial galvanostatic cycling behavior of the composite graphite is shown in Fig. 2. Note that the capacity was based on the total weight of the electrode. According to previous results, the region between 1.1 and 0.56 V versus Li/Li$^+$ denoted as region A in the figure, corresponds to the electrolyte decomposition/SEI layer formation [5]. The reactions occurring during solvent decomposition, in a mixture of EC and DMC solvents is given by the reactions

$$2Li^+ + EC \rightarrow Li_2CO_3 + CH_2CH_2(g)\uparrow$$

$$2Li^+ + DMC \rightarrow Li_2CO_3 + CH_3CH_3(g)\uparrow$$

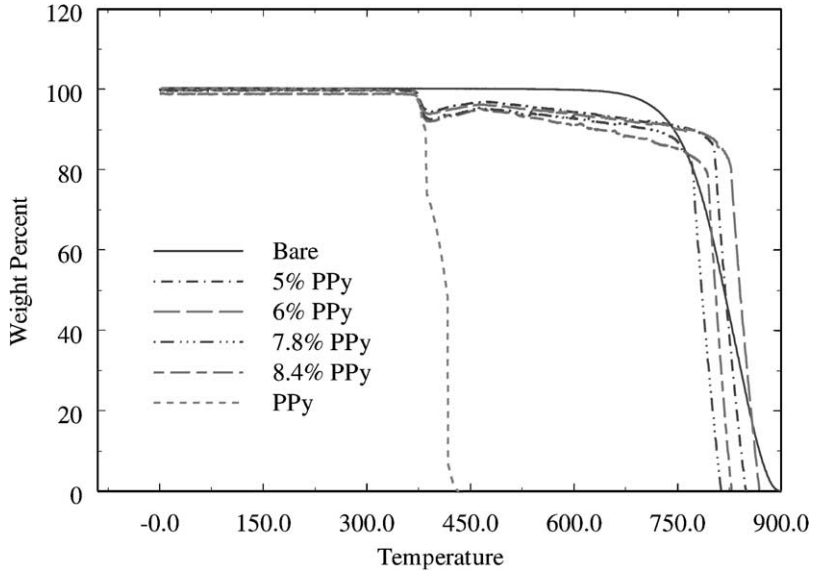

Fig. 1. TGA analysis of bare and PPy/C composites at a scan rate of 5 °C/min under air atmosphere.

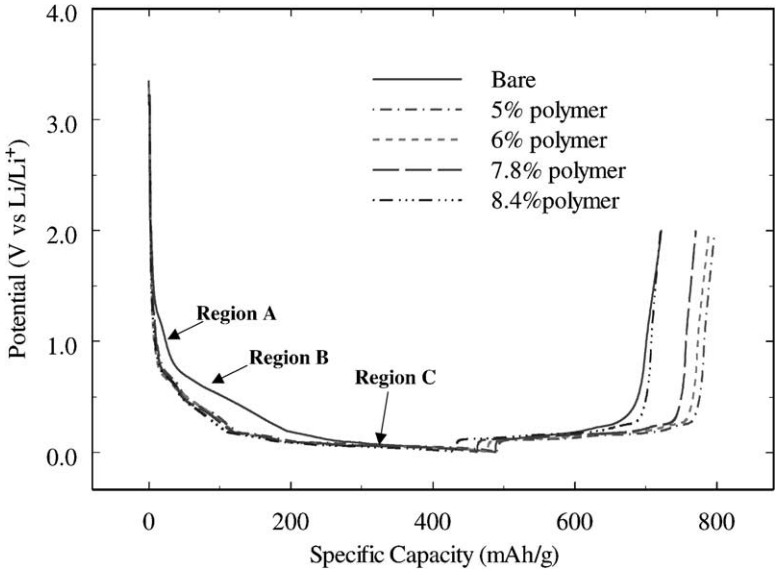

Fig. 2. Initial galvanostatic charge–discharge curves of bare and polypyrrole composite SFG10 samples in 1 M $LiPF_6$/EC/DMC electrolyte at *C*/15 rate.

The region between 0.56 and 0.2 V versus Li/Li^+ is mainly associated with the solvated lithium intercalation and subsequent reduction of the electrolyte, denoted by the region B in Fig. 2 [24]. The region below 0.2 V versus Li/Li^+, denoted as region C in Fig. 2, is associated with the reversible lithium–graphite intercalation compound (Li–GIC) formation. For bare SFG10, the irreversible capacity loss arising due to reactions in regions A and B is 253.2 mAh/g. The coulombic efficiency in the first cycle is 47.9%. The huge irreversible capacity associated with the SFG10 graphite maybe due to its large surface area [24]. However, in the case of polypyrrole composite graphite, the plateaus due to both these irreversible reactions are reduced as seen in Fig. 2. Note that in the case of the composite graphites, the reduction in the plateau due to SEI layer formation (region A) is more when compared to the reduction in the solvated intercalation plateau (region B). Such a behavior indicates that polypyrrole acts as a film that reduces the activity of the graphite surface thus reducing the irreversible reactions with the electrolyte, while the lithium intercalation (and hence the solvated lithium intercalation) inside the graphene layers are not inhibited. These results show that addition of polypyrrole is favorable for reducing the irreversible reactions of graphite.

Table 1 presents the irreversible capacity loss in the composite and the bare graphite for various loading of polypyrrole on graphite. From the table, it can be seen that the initial irreversible capacity loss associated with bare SFG10 is 52.1%. The amount of irreversible capacity loss decreases with increase in polypyrrole content, up to a composition of 7.8 wt.% PPy, to the tune of 32.1%. The reason for this is that addition of polypyrrole results in the formation of a matrix in which the graphite particles are binded together. Polypyrrole being a conducting polymer when doped, its addition results in an increase of the conductivity of the samples and a decrease in the particle-to-particle resistance. The first cycle coulombic efficiency of the composite electrodes also shows a similar behavior with the addition of polypyrrole, where it increases from 47.9% in the case of virgin graphite to 67.9% in the case of PPy/C composite. However, from the table, it can be seen that the PPy loading of 7.8 wt.% represents the optimum concentration and further increase in polypyrrole only serves to add to the dead weight of the battery.

Table 1
Initial irreversible capacity loss of the composites at *C*/15 rate as a function of the polypyrrole content

Amount of PPy loading (wt.%)	Initial lithiation capacity (mAh/g)	Initial de-lithiation capacity (mAh/g)	Total irreversible capacity loss[a] (%)	Initial coulombic efficiency (%)
0	485.9	232.7	52.1	47.9
5	483.7	309.3	36.1	63.9
6	471.7	313.6	33.5	66.5
7.8	456.6	310.1	32.1	67.9
8.4	432.5	290.3	32.9	67.1

[a] Total irreversible capacity loss = [(initial lithiation capacity − initial de-lithiation capacity)/initial lithiation capacity] × 100.

3.3. Cyclic voltammograms

Kinetics of Li intercalation in the composite can be studied using cyclic voltammograms (CVs). CVs were obtained at a slow scan rate of 0.05 mV/s. The potential was swept from 1.6 to 0.01 versus Li/Li^+ in the cathodic direction and back to 1.6 V in the anodic direction. This potential range covered all the irreversible interactions between the host, lithium, and the electrolyte and also the lithium intercalation reaction into the composites. This potential range is also representative of the processes occurring at the anode under normal battery operating conditions. It is worth noting that when polypyrrole alone was cycled in this potential range, the currents obtained was negligible. This clearly shows that polypyrrole has no electrochemical activity towards lithium intercalation in this potential range, although some activity has been reported for polypyrrole prepared through electrochemical means in the potential range typical for cathodes (2.5–4.2 V versus Li/Li^+) [21]. Since polypyrrole showed no activity, the observed reduction in the irreversible capacity could be due to fewer exposed edges as the polypyrrole binds the graphite particles. Fig. 3 shows the cyclic voltammogram of composite SFG10 graphites. The cyclic voltammogram performed on the bare graphite has also been shown for comparison. Sweeping the potential from 1.6 V to 0.01 V results in lithiating the composite. Kinetics of Li intercalation for all the samples remains low till 1.1 V. Beyond this, a sharp increase in the current is seen. According to Gnanaraj et. al. [25], electrolyte decomposition starts at a potential of 1.1 V versus Li/Li^+ and continuous reduction of the solvent molecules and the formation of the ionically conducting and electronically insulating SEI layer occurs till a potential of 0.56 V. According to Winter et. al. [24], the solvated lithium intercalation and subsequent reduction of the electrolyte molecules inside the graphene layers occurs in the potential range of 0.56–0.2 V versus Li/Li^+. Fig. 3 also shows a reduction in the currents associated with both these reactions in the case of the composite graphites. During de-intercalation (sweeping the voltage from 0.01 to 1.6 V) two characteristic peaks corresponding to the de-intercalation of the lithium ion from the anode material appear at the same voltage for all the samples. However, the magnitude of the peak current has increased for PPy/C composite. Comparison of the ratio of charges under the anodic and cathodic sweeps reveals a higher coulombic efficiency for the composite graphite samples. The numerical values for the irreversible capacity loss and the coulombic efficiency from CV data were obtained by integrating the *I–V* curves.

Integrating the area under the cathodic curve from 1.6 to 0.2 V yields the total irreversible capacity from the CV data. Such integration will give corroboration for the results obtained in the charge–discharge studies. The results obtained from the CV data have been presented in Table 2. The data shows that the lithium intercalation capacity for the bare graphite material is 271.7 mAh/g, which is comparable to the irreversible capacity seen in the case of charge–discharge studies. The integration of the *I–V* curves for the composites yielded similar results as seen in the case of charge–discharge studies. The total irreversible capacity is reduced to 149.6 mAh/g in the case of the 7.8% PPy/C composite. The coulombic efficiency also increases from 45.9 to 66.9%. The data obtained from the CVs also shows that the optimum PPy concentration is 7.8 wt.%, which is consistent with the result obtained in charge–discharge studies. The improved capacity maybe due to the increase in the conductivity of the samples and reduction in the particle-to-particle resistance. The next set of studies was done to investigate the reasons responsible for these observations.

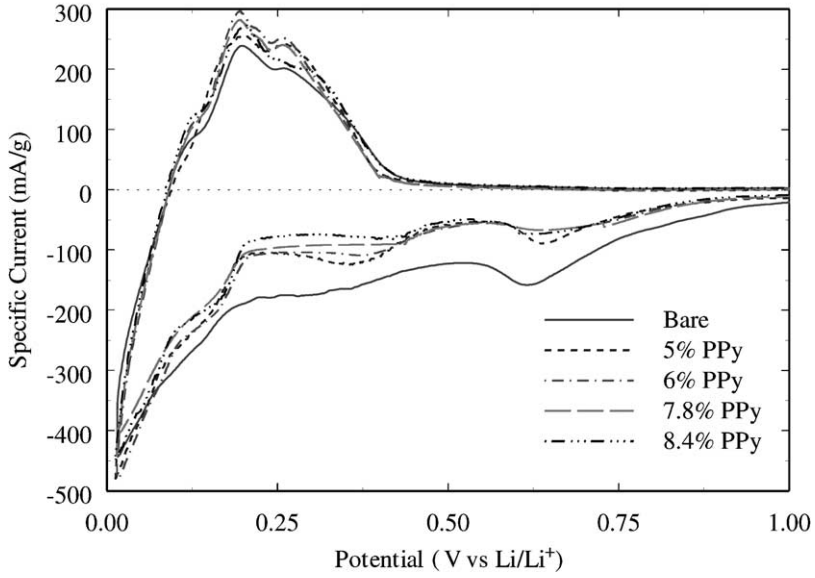

Fig. 3. Cyclic voltammograms of bare and polypyrrole composite SFG10 samples in 1 M $LiPF_6$/EC/DMC electrolyte at 0.05 mV/s.

Table 2
Initial irreversible capacity loss of the composites calculated from cyclic voltammograms as a function of polypyrrole content in the composites

Amount of PPy loading (wt.%)	Initial lithiation capacity (mAh/g)	Capacity between 1.6 and 0.2 V vs. Li/Li^+ (mAh/g)	Total irreversible capacity loss[a] (%)	Initial coulombic efficiency (%)
0	502.5	271.7	54.1	45.9
5	479.3	166.5	34.7	65.3
6	493.5	167.7	34.0	66.0
7.8	452.4	149.6	33.1	66.9
8.4	442.4	149.5	33.8	66.2

[a] Total irreversible capacity loss = [(capacity between 1.6 and 0.2 V vs. Li/Li^+)/initial lithiation capacity] × 100.

Table 3
Comparison of the reversible capacities of PPy/C samples and bare graphite material (SFG10) at *C*/15 rate

Amount of Ppy loading (wt.%)	Reversible capacity (mAh/g)	Specific surface area (m^2/g)	Volumetric surface area (m^2/cm^3)	Volumetric capacity (mAh/cm^3)
0	284.6	9.84	21.65	626.1
5	338.8	8.98	19.76	745.4
6	359.8	8.55	18.81	791.6
7.8	362.3	7.78	17.12	797.1
8.4	359.0	7.69	16.92	789.8

Table 3 presents the BET results and the effect of polypyrrole addition on the reversible capacity of the samples. The BET results show that the addition of polypyrrole reduces the surface area of the samples. The reduction in surface area increases with increase in the polypyrrole content in the samples. The reduction of the surface area in the samples, thus confirms that the observed lowering of the irreversible capacity loss is due to the reduction in the exposed edges. However, it has to be mentioned that polypyrrole only reduces the exposed surface edges, since the specific capacity is not affected adversely and in fact, improves. This is further confirmed by the increase of the volumetric capacity despite a reduction of the volumetric surface area (see Table 3). However, as mentioned in the CV results, cycling polypyrrole alone did now show any significant current, emphasizing the fact that polypyrrole does not contribute to the capacity. So, the observed improvements in the electrochemical characteristics should arise because of the better conductivity of the composites. To investigate this further, electrochemical impedance spectroscopy (EIS) studies were done.

3.4. Influence of polypyrrole addition on conductivity

The conductivity of electrode material is a very important factor in evaluating the high rate performance of the

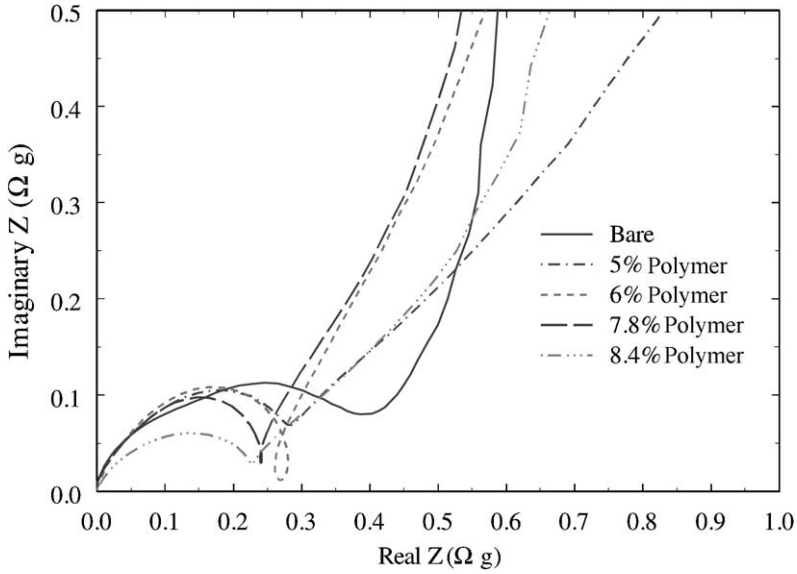

Fig. 4. Impedance plots for the bare and polypyrrole composite SFG10 graphite in the de-lithiated state.

batteries. Impedance analysis was done to study the various resistances of composite graphite. Fig. 4 shows the Nyquist plots for the impedance response of composite electrode. Impedance of the anode in the Li-ion cell depends strongly on the lithium content inside these electrodes. To maintain uniformity, all the impedance analyses were done on completely charged samples (state of charge = 100%). The electrodes underwent 15 charge–discharge cycles to ensure the complete formation of the SEI layer. The polarization resistance of polypyrrole composite SFG10 decreases with an increase in the polypyrrole content in the composite. The curves shown in Fig. 4 are composed of two overlapping depressed semi-circles. According to previous studies, the high frequency semi-circle corresponds to the migration of the Li ions through a surface film at the electrode/electrolyte interface and the second semi-circle appearing at a lower frequency is attributed to the charge transfer kinetics [26]. Fig. 4 show that the addition of polypyrrole reduces the semi-circle part of the impedance. However, the decrease of the high frequency semi-circle part is more prominent than the second semi-circle. This result indicates that the resistance posed by the passive film to the migration of lithium ion is reduced for the composites. To understand this phenomenon better, the experimental impedance data was fitted to an equivalent circuit.

Fig. 5 shows the circuit used to fit the experimental impedance responses shown in Fig. 4. Fitting the experimental impedance plot to the equivalent circuit will provide important information about the changes in the polarization resistance and the SEI layer characteristics due to the addition of polypyrrole. As there were two separate processes involved in the transport of the lithium ion, two separate combinations of R and C components were used in the equivalent circuit. A single resistance in the front represented the solution resistance. The differential elements in the equivalent circuit were used for compensating the non-ideal nature of the semi-circles. The numerical values for the different components were obtained by fitting the experimental results and are given in Table 4. As seen from the table, addition of polypyrrole does not have much effect on the components responsible for the faradaic reaction. This means that polypyrrole addition does not alter the catalytic properties of the material. However, it can be seen that the SEI layer resistance is decreased by two orders of magnitude, while the SEI layer capacitance was found to increase by at least two orders of magnitude based on the fitting results (values not shown here). This result shows that the thickness of the SEI layer is decreased remarkably in the case of the composite graphites. The reduction of the SEI layer formed can be directly correlated to the decrease in the irreversible capacity seen in the case of the composite graphites. This result also serves as a confirmation to the reasoning that addition of polypyrrole reduces the exposed surface edges to the electrolyte, which translates into reduction in the thickness of the SEI layer formed in the composites.

Table 4
Electrode resistance obtained from equivalent circuit fitting of experimental data

Sample	R_Ω (Ω g)	R_1 (Ω g)	R_2 (Ω g)
Bare	0.14	3.6	0.3
5% PPy	0.13	0.5	0.3
6% PPy	0.13	0.4	0.2
7.8% PPy	0.14	0.3	0.2
8.4% PPy	0.14	0.1	0.2

The studies done so far reveal that the lowest irreversible capacity loss is obtained in the case of 7.8 wt.% PPy/C electrodes. Polypyrrole addition also increases the coulombic efficiency of the composite electrode. Fig. 6 shows a comparison in the coulombic efficiencies of bare and 7.8 wt.% polypyrrole composite electrodes. As seen from the figure, bare SFG10 electrode has poor coloumbic efficiency in the first discharge cycle owing to the irreversible reactions happening on the electrode. On the other hand, the coloumbic efficiency is comparatively higher for polypyrrole composite electrodes owing to minimized irreversible reactions. After the initial cycle, the polypyrrole-coated composites are more stable in the electrolyte and the irreversible reactions are completed within the first three cycles. This is supported by the near 100% efficiency for the PPy-composites from the third cycle while for the bare graphite, it takes about 10 cycles to achieve near 100% coloumbic efficiency. All these results indicate that the composite electrodes gives better performance than the bare graphite.

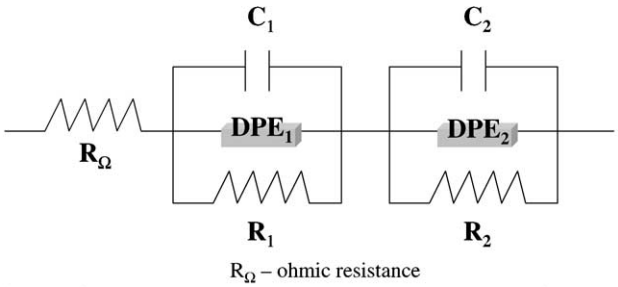

Fig. 5. Equivalent circuit used to fit the experimental impedance responses of the composites.

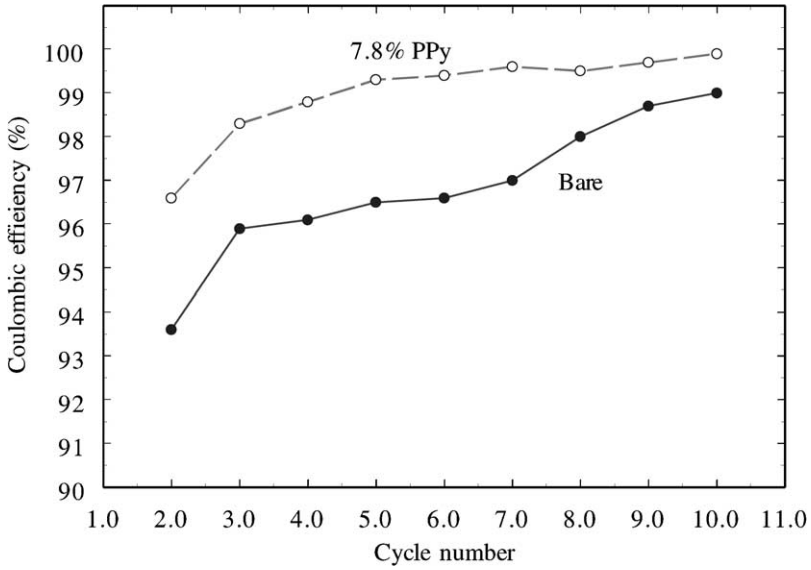

Fig. 6. Coulombic efficiency of bare and 7.8 wt.% composite SFG10 samples for the first 10 cycles at *C*/15 rate.

Rate capability studies were done on the samples to ascertain the performance of the materials under varying load conditions. Fig. 7 gives the discharge capacity of different samples at various applied load conditions. All the capacities reported on the graph correspond to the de-intercalation capacity, i.e. the charge capacity. A look at the figure shows that the composite graphite gives consistently higher capacity at all rates compared to the bare graphite. At an applied load corresponding to a rate of *C*/15, the bare graphite gives 81% of the theoretical capacity (301 mAh/g). As the rate is increased, the performance of the bare graphite decreases drastically. When the rate is increased to *C*/6, the capacity drops down to 226 mAh/g, reaching a value of 61% of the theoretical capacity. The capacity further falls to 128.1 mAh/g at *C*/3 rate, giving just 34.4% of the theoretical capacity and reaching a value of 58.6 mAh/g at *C* rate, consisting only 15.8% of the theoretical capacity. This indicates the dependence of lithium intercalation on the mass transfer inside the electrode. Also, the conductivity of the electrode plays an important role in determining the high rate performance. The composite graphite sample shows remarkable improvement in the performance of the graphite. As shown in the previous studies, addition of polypyrrole improves the conductivity of the composite electrode and reduces the particle-to-particle contact resistance. When the composite graphite was subjected to rate capability studies it showed negligible reduction (<20 mAh/g) in the capacity due to increase in the load up to *C*/3 rate.

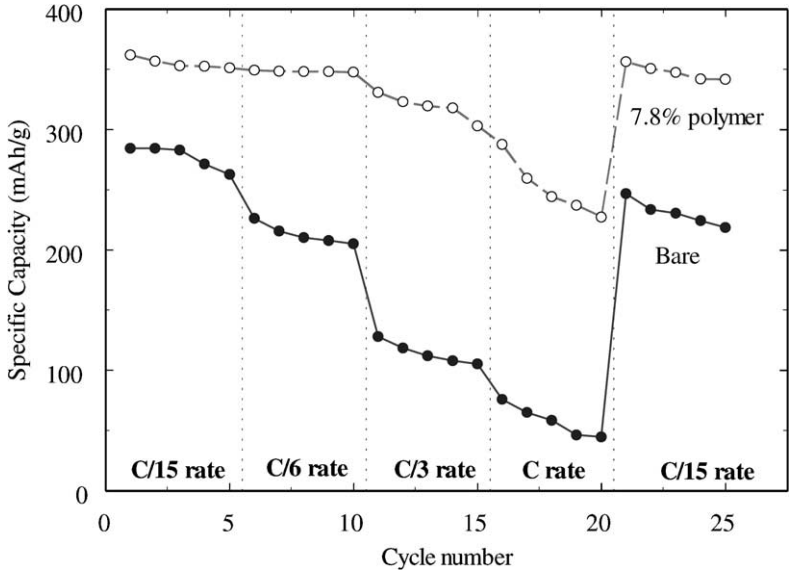

Fig. 7. Rate capability studies of bare and 7.8 wt.% composite SFG10 samples.

When the discharge current was increased to C rate, the composite graphite showed a reduction in the capacity to 259.7 mAh/g. However, a comparison to the bare graphite under a similar load shows that the composite graphite gives approximately five times the capacity of the bare graphite at C rate. The improved conductivity, as seen by EIS data, can be the main reason behind the better rate capability of the composite electrode.

3.5. Cycle life studies

Polypyrrole is a well-known conducting polymer, which has been used in rechargeable lithium batteries as a positive electrode in conjunction with Li or carbon electrodes. Previous studies show that the material is stable in the organic electrolyte used in Li-ion cells. Kuwabata et al. have studied the effect of polypyrrole addition on Li-ion cathode materials such as $LiMn_2O_4$ [22] and V_2O_5 [23]. During these studies, they investigated the electrochemical stability of polypyrrole in a 1:1 mixture of EC:DEC with 1 M $LiClO_4$ using cyclic voltammetry. No additional peaks due to polypyrrole redox reaction were seen during the anodic scan. Voltammetric studies done by us on pure polypyrrole electrodes in the organic electrolyte reveal no electrochemical activity indicating that the material is inert to oxidation and hence is electrochemically stable. Further charge–discharge studies conducted by Kuwabata et al. [22,23] reveal no loss in capacity with cycling for the composite electrodes. Boinowitz et al. [27] have studied the performance of polypyrrole as a negative electrode in a novel metal-free battery using $LiClO_4$ and PC electrolyte. They too report no adverse effects on the stability of the material in organic electrolyte. These studies indicate that polypyrrole is chemically stable in Li-ion battery electrolytes. To check the stability of the composite material in Li-ion environment, extended cycling studies were done on T-cells containing bare and surface modified SFG10 working electrodes. Fig. 8 shows the discharge capacity of the composite and bare graphite after the first cycle. From the graph, we can see that the composite displays a constant capacity during cycling. The better conductivity of the sample leads to better utilization of the material in the case of the composites and hence results in higher capacity for the composite material. The study also reveals that the composite material is stable in the organic electrolyte.

In our previous study, we deposited amorphous Sn on SFG10 graphite, which improved the specific capacity of the material significantly. We had optimized 15% Sn as the optimum concentration based on the discharge capacity of the composite. However, the drawback of the Sn/C composite was that it showed higher irreversible capacity than bare SFG10 graphite, due to the irreversible reduction of SnO_2 to Sn in the initial cycle. The reaction is given by Courtney and Dahn [7] as

$$SnO_2 + Li \rightarrow Sn + LiO_2$$

Since, polypyrrole addition results in the reduction in irreversible capacity seen in the case of the bare SFG10 graphite, we wanted to study the effect of polypyrrole addition on Sn/C composite. Fig. 9 shows the charge–discharge behavior of the Sn/C and the Sn/PPy/C composite. The graph shows a remarkable decrease in the irreversible capacity associated with the Sn/C composite. Analysis of the potential profile shows for the Sn/C composite that after SEI layer formation, more capacity is utilized in the region 0.56–0.2 V for Sn/C composites than for the bare graphite. This is due to the reduction of SnO_2 to Sn. However, the Sn/PPy/C composite shows much lower irreversible capacity than Sn/C composite. The plateau due to SEI layer formation is seen to decrease even in the case of Sn/PPy/C composite.

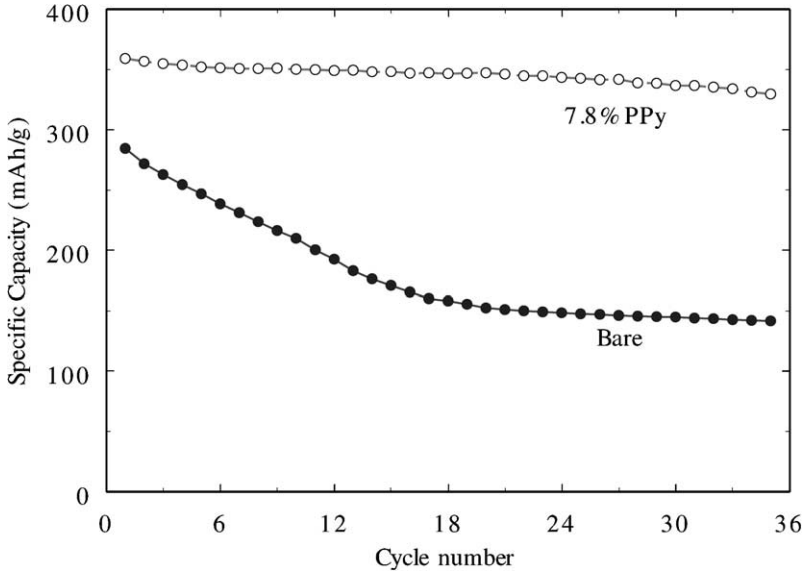

Fig. 8. Cycle life studies of bare and 7.8 wt.% composite SFG10 samples at *C*/15 rate.

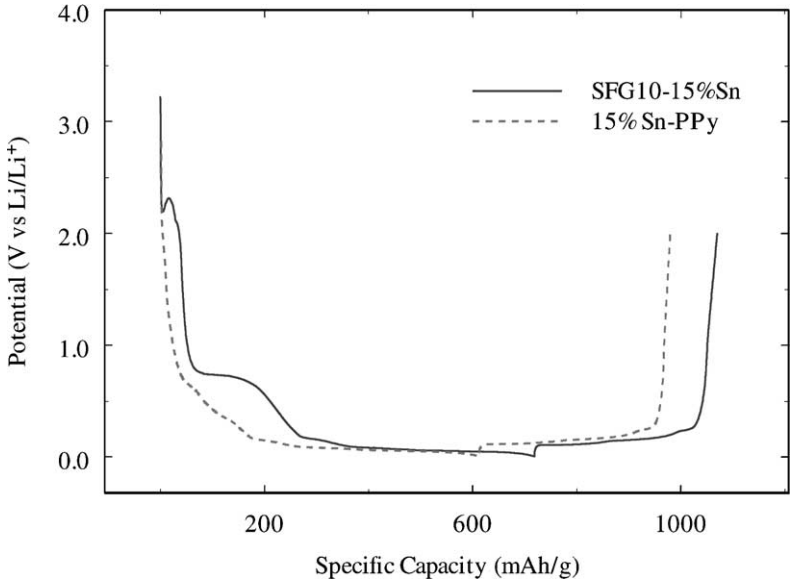

Fig. 9. Initial galvanostatic charge–discharge curves of 15 wt.% Sn composite SFG10 and polypyrrole treated 15 wt.% Sn/C SFG10 samples at *C*/15 rate.

However, the plateau due to the reduction of the SnO_2 to Sn and solvated lithium intercalation is still significant in the case of the Sn/PPy/C composite.

Comparison between the irreversible capacities of the bare and the Sn/C composite will give an estimate of the irreversible capacity due to the addition of tin. The irreversible capacity due to Sn in the case of Sn/C composite is found to be 115.9 mAh/g. Comparison between the irreversible capacity of the PPy/C composite and the Sn/PPy/C composites gives an estimate of the irreversible capacity due to tin in the case of Sn/PPy/C composite to be 89.3 mAh/g, which is comparable to the irreversible capacity due to tin in the case of Sn/C composite. This result shows that addition of polypyrrole has an effect of reducing the surface area and hence the irreversible capacity and does not alter the catalytic activity of the electrode material.

4. Conclusions

Pyrrole was polymerized onto commercial graphite, Timcal SFG10, to form PPy/C composites suitable for use as negative electrodes in Li-ion cells. At levels up to 7.8 wt.% PPy, the irreversible capacities of the composites during galvanostatic cycling are significantly decreased relative to the bare graphite. At a *C*/15 rate, an irreversible capacity of 146.5 mAh/g is obtained for PPy/C composite, compared to 253.2 mAh/g for the uncoated graphite, a decrease of over 20%. The reversible capacities are also increased for the composite graphites, increasing from 284.6 mAh/g for the bare graphite to 362.3 mAh/g for a PPy concentration of 7.8 wt.%. Cyclic voltammetric experiments corroborated the galvanostatic cycling tests, with composite graphites showing lower peak currents due to SEI layer formation and the solvated lithium intercalation reaction and lower irreversible capacities relative to the bare control material. Additional confirmation was obtained through complex-impedance spectroscopy. Addition of polypyrrole to the graphite reduces the charge-transfer resistance and overall polarization resistance, very likely by reducing the amount of SEI formation. This is corroborated by fitting the impedance results to an equivalent circuit. The composite graphite sample also showed very good rate capability, coulombic efficiency and cycling behavior, compared to the virgin carbon. Finally, addition of polypyrrole to Sn/C composite reduced the irreversible capacity of these composites. Current efforts are concentrated on further reduction of the irreversible capacity associated with these composites.

Acknowledgements

This research was carried out under a contract with the National Reconnaissance Office for Hybrid Advanced Power Sources #NRO-00-C-1034. This material is also based upon work supported by the National Science Foundation under Grant No. 0097701.

References

[1] M.B. Armand, in: D.W. Murphy, J. Broadhead, B.C. Steele (Eds.), Material for Advanced Batteries, Plenum Press, New York, 1980, p. 145.
[2] D. Guymard, J.M. Tarascon, J. Electrochem. Soc. 139 (1992) 937.
[3] T. Zheng, Q. Zhong, J.R. Dahn, J. Electrochem. Soc. 142 (1995) L211.
[4] P. Arora, R.E. White, M. Doyle, J. Electrochem. Soc. 145 (1998) 3647.
[5] W. Xing, J.R. Dahn, J. Electrochem. Soc. 144 (1997) 1195.
[6] B. Veeraraghavan, A. Durairajan, B. Haran, B.N. Popov, J. Electrochem. Soc. 149 (6) (2002) 1.

[7] I.A. Courtney, J.R. Dahn, J. Electrochem. Soc. 144 (1997) 2045.
[8] R. Fong, U. von Sacken, J.R. Dahn, J. Electrochem. Soc. 137 (1990) 2009.
[9] K. Takei, K. Kumai, Y. Kobayashi, H. Miyashiro, T. Iwakori, T. Uwai, H. Ue, J. Power Sources 54 (1995) 171.
[10] T. Osaka, T. Momma, Y. Matsumoto, Y. Uchida, J. Electrochem. Soc. 144 (1997) 1709.
[11] F. Kong, J. Kim, X. Song, M. Inaba, K. Kinoshita, F. McLarnon, Electrochem. Solid State Lett. 1 (1998) 39.
[12] M. Arakawa, J. Yamaki, J. Electroanal. Chem. 219 (1987) 273.
[13] G.C. Chung, S.H. Jun, K.Y. Lee, M.H. Kim, J. Electrochem. Soc. 146 (1999) 1664.
[14] O. Chusid, Y. Ein-Eli, D. Aurbach, J. Power Sources 43/44 (1993) 47.
[15] J.O. Besenhard, M.W. Wagner, A.D. Jannakoudakis, P.D. Jannakoudakis, E. Theodoridou, J. Power Sources 43/44 (1993) 413.
[16] Y. Ein-Eli, S.R. Thomas, V.R. Koch, J. Electrochem. Soc. 143 (1996) L195.
[17] P. Yu, J.A. Ritter, R.E. White, B.N. Popov, J. Electrochem. Soc. 147 (2000) 1280.
[18] P. Yu, B.S. Haran, J.A. Ritter, R.E. White, B.N. Popov, J. Power Sources 91 (2000) 107.
[19] L.W. Shacklette, T.R. Jow, M. Maxfield, R. Hatami, Synth. Metals 28 (1989) C655.
[20] M.G. Kanatzidis, Chem. Eng. News 68 (1990) 36.
[21] A.D. Pasquier, F. Orsini, A.S. Gozdz, J.M. Tarascon, J. Power Sources 81/82 (1999) 607.
[22] S. Kuwabata, S. Masui, H. Yoneyama, Electrochim. Acta 44 (1999) 4593.
[23] S. Kuwabata, S. Masui, H. Tomiyori, H. Yoneyama, Electrochim. Acta 46 (2000) 91.
[24] M. Winter, P. Novak, A. Monnier, J. Electrochem. Soc. 145 (1998) 428.
[25] J.S. Gnanaraj, M.D. Levi, E. Levi, G. Salitra, D. Aurbach, J.E. Fischer, A. Claye, J. Electrochem. Soc. 148 (2001) 525.
[26] D. Aurbach, M.D. Levi, E. Levi, H. Teller, B. Markovsky, G. Salitra, U. Heider, L. Heider, J. Electrochem. Soc. 145 (1998) 3024.
[27] T. Boinowitz, G. Suden, U. Tormin, H. Krohn, F. Beck, J. Power Sources 56 (1995) 179.